Chaos, Solitons and Fractals 150 (2021) 111116

Contents lists available at ScienceDirect

Chaos, Solitons and Fractals

Nonlinear Science, and Nonequilibrium and Complex Phenomena

journal homepage: www.elsevier.com/locate/chaos

Robust and accurate construction of the local volatility surface using the Black–Scholes equation

Sangkwon Kim, Junseok Kim*

Department of Mathematics, Korea University, Seoul 02841, Republic of Korea

ARTICLE INFO

Article history:
Received 29 March 2021
Revised 11 May 2021
Accepted 27 May 2021
Available online 18 June 2021

Keywords:
Local volatility surface
FDM
Nonlinear curve-fit
Option pricing

ABSTRACT

In this study, we develop a numerical method for the robust and accurate construction of a local volatility (LV) surface using the generalized Black–Scholes (BS) equation from the given option price data. The BS equation is a partial differential equation and has been used to model financial option pricing. Constant volatility was used in the classical BS model. However, it is well known that the constant volatility BS model is practically unsuitable because real financial market data demonstrate non-constant volatility behavior. The LV function is dependent on the asset prices and time. One of the difficulties in reconstructing an unknown LV surface is uniqueness. We extend a previous study of reconstructing time-dependent volatility, which is unique, to time- and space-dependent volatility surfaces. We propose an algorithm comprising four steps: the first step is estimating constant implied volatility; the second step is finding the influential region using the probability density function of a log-normal distribution; the third step is calculating the time-dependent volatility function; and the final step is reconstructing the LV surface. We use a finite difference method to numerically solve the BS model and a nonlinear fitting function to compute the LV surface. We perform computational experiments using synthetic and real market data. The numerical results demonstrate the robust and accurate construction of an unknown LV surface using the proposed method.

1. Introduction

In this article, we present a numerical method for the robust and accurate construction of a local volatility (LV) surface using the generalized Black–Scholes (BS) equation [1,2]. The BS equation is a partial differential equation and has been used to model financial option pricing. Constant volatility has been used in the classical BS model [3]. Let S be the underlying price, t be time, and $u(S,t)$ be the option price. The classical form of the BS equation is as follows:

$$\frac{\partial u(S,t)}{\partial t}+\frac{1}{2}[\sigma S]^2\frac{\partial^2 u(S,t)}{\partial S^2}+rS\frac{\partial u(S,t)}{\partial S}-ru(S,t)=0, \quad \text{for } (S,t)\in\mathbb{R}^+\times[0,T), \tag{1}$$

where σ is the constant volatility, r is the risk-free rate, and T is the final time. The terminal condition is $u(S,T)=\Lambda(S)$ at $t=T$, where $\Lambda(S)$ is a function that depends on the financial option types [3]. For example, $\Lambda(S)=\max(S-K,0)$ for a European call option with strike price $K=100$, as shown in Fig. 1.

However, it is well known that the constant volatility BS model is practically unsuitable because real financial market data demonstrate non-constant volatility behavior. Therefore, we should consider the following generalized BS equation:

$$\frac{\partial u(S,t)}{\partial t}+\frac{1}{2}[\sigma(S,t)S]^2\frac{\partial^2 u(S,t)}{\partial S^2}+rS\frac{\partial u(S,t)}{\partial S}-ru(S,t)=0, \tag{2}$$

where $\sigma(S,t)$ is the LV function that depends not only on the underlying asset S, but also on time t. Some studies have focused on reconstructing only the time-dependent volatility function using market option data [4,5]. The LV model was introduced by Dupire [6] and Derman and Kani [7] for pricing and managing the risks of options. Numerous studies have been conducted on the effects of $\sigma(S,t)$ [8–12]. Itkin [13] emphasized the need for more research on LV in mathematical finance. The study covers numerical approaches for interpolating and extrapolating the LV surfaces. Many studies on constructing the LV surface using calibration methods have been conducted. Guo et al. [14] used the optimal transport and alternative direction method of multipliers (ADMM) algorithm to construct the LV function. However, the algorithm exhibited a slow convergence rate. Lim [15] used a linear function to estimate the transition probability function to construct a volatility surface. Xu and Jia [16] proposed a calibration method by solving an in-

* Corresponding author.
E-mail address: cfdkim@korea.ac.kr (J. Kim).

https://doi.org/10.1016/j.chaos.2021.111116
0960-0779/

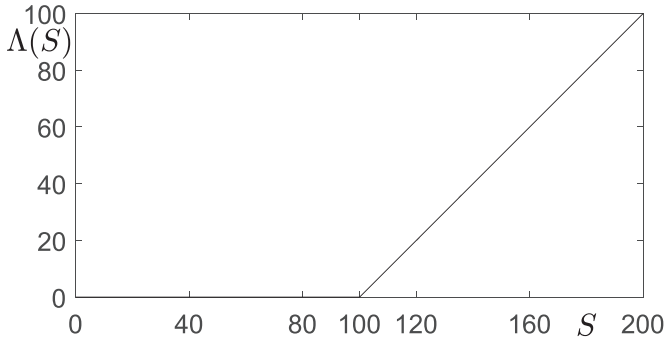

Fig. 1. Payoff function $\Lambda(S) = \max(S - K, 0)$ for a European call option with a strike price $K = 100$.

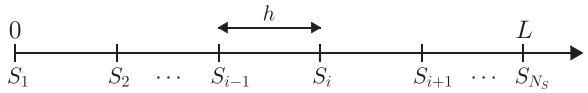

Fig. 2. Uniform grid with the space step h.

verse problem using an iterative algorithm. The algorithm was applied to the jump-diffusion model, and tests with different conditions showed the robustness of the proposed method. Ogetbil et al. [17] proposed a Monte Carlo simulation algorithm. A disadvantage is that the Monte Carlo method requires a high computational cost to achieve high accuracy. Santos [18] analyzed the problem within a time-transformation framework. Using additional information, the authors improved the performance of the Bayesian methods.

This study primarily aims to develop a robust and accurate numerical method for reconstructing an unknown LV surface using the BS equation and the observed real market European call option prices.

The remainder of this paper is organized as follows. In Section 2, the proposed numerical algorithm for constructing the LV surface is described. In Section 3, numerical experiment results are presented, and the conclusions are drawn in Section 4.

2. Numerical algorithm

By changing the variable to $\tau = T - t$, Eq. (2) can be given as follows:

$$\frac{\partial u(S,\tau)}{\partial \tau} = \frac{1}{2}[\sigma(S,\tau)S]^2 \frac{\partial^2 u(S,\tau)}{\partial S^2} + rS\frac{\partial u(S,\tau)}{\partial S} - ru(S,\tau), \quad (3)$$

for $(S,\tau) \in \Omega \times (0,T]$. Here, we redefined $u(S, T-\tau)$ as $u(S,\tau)$ for simplicity of notation. The initial condition is the payoff function, $u(S,0) = \Lambda(S)$ for $S \in \Omega = (0, L)$, where the infinite domain is truncated to a finite computational domain [19]. Using the implicit Euler method in Eq. (3), we obtain

$$\frac{u_i^{n+1} - u_i^n}{\Delta\tau} = \frac{(\sigma_i^{n+1}S_i)^2}{2}\frac{u_{i-1}^{n+1} - 2u_i^{n+1} + u_{i+1}^{n+1}}{h^2} + rS_i\frac{u_{i+1}^{n+1} - u_{i-1}^{n+1}}{2h} - ru_i^{n+1}. \quad (4)$$

Let us denote the numerical approximation of the solution by $u_i^n \equiv u(S_i, \tau_n) = u(ih,\ n\Delta\tau)$ and the discrete volatility function $\sigma_i^n \equiv \sigma(S_i, \tau_n)$ for $i = 1, 2, \ldots, N_S$ and $n = 0, 1, \ldots, N_\tau$, where N_S and N_τ are the number of grid points and time steps, respectively. Here, uniform space and time steps are $h = L/(N_S - 1)$ and $\Delta\tau = T/N_\tau$, respectively. Fig. 2 shows a schematic of a uniform grid with space step h.

We can rewrite the above Eq. (4) as

$$\alpha_i u_{i-1}^{n+1} + \beta_i u_i^{n+1} + \gamma_i u_{i+1}^{n+1} = b_i, \quad \text{for } i = 2, \ldots, N_S, \quad (5)$$

$$\alpha_i = \frac{rS_i}{2h} - \frac{(\sigma_i^{n+1}S_i)^2}{2h^2}, \quad \beta_i = \frac{1}{\Delta\tau} + \frac{(\sigma_i^{n+1}S_i)^2}{h^2} + r,$$

$$\gamma_i = -\frac{rS_i}{2h} - \frac{(\sigma_i^{n+1}S_i)^2}{2h^2}, \quad b_i = \frac{u_i^n}{\Delta\tau}.$$

The boundary condition is set as the zero Dirichlet and the linear boundary condition at S_1 and S_{N_S}, respectively, that is, $u_1^n = 0$ and $u_{N_S+1}^n = 2u_{N_S}^n - u_{N_S-1}^n$ for all n [20]. We apply the Thomas algorithm [21] to solve the resulting discrete system (5).

2.1. Reconstruct volatility surface

In this section, we propose an algorithm for reconstructing the LV surface. We define the cost function $\mathcal{E}(\sigma)$, which is defined as:

$$\mathcal{E}(\sigma) = \frac{1}{M_t M_k}\sum_{\alpha=1}^{M_t}\sum_{\beta=1}^{M_k}[u_{K_\beta}(\sigma; S_0, T_\alpha) - V_\beta^\alpha]^2\chi_\beta^\alpha, \quad (6)$$

where if V_β^α is available, a characteristic function $\chi_\beta^\alpha = 1$; otherwise, $\chi_\beta^\alpha = 0$, the numerical solution $u_{K_\beta}(\sigma; S_0, T_\alpha)$ at $S = S_0$ in Eq. (3) and the market value V_β^α of European options with the strike price K_β for $\beta = 1, \ldots, M_k$ at maturity time T_α for $\alpha = 1, \ldots, M_t$. Here, T_α and K_β increase with increasing subscripts, that is, $T_1 < \ldots < T_{M_t}$ and $K_1 < \ldots < K_{M_k}$. The proposed algorithm comprises the following four steps: *Step 1*: We estimate the constant implied volatility σ_{im} by using the exact formula of the call option price and *lsqcurvefit* [22]. In MATLAB, *lsqcurvefit* is a nonlinear

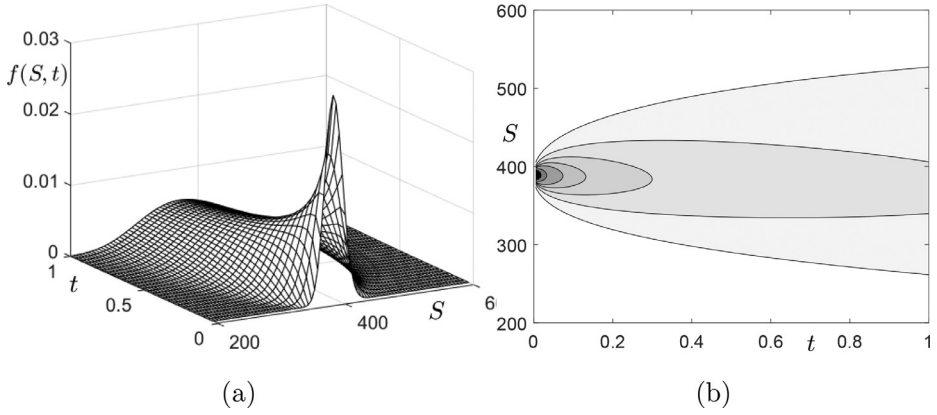

Fig. 3. (a) Log-normal distribution PDF. (b) Contour plot at levels $f = 0.001, 0.005, 0.01, 0.015, 0.02, 0.03, 0.04, 0.5$.

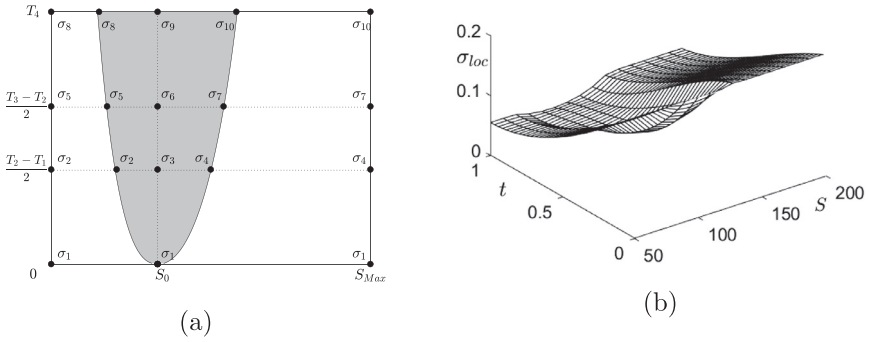

Fig. 4. Schematic illustrations of (a) position of unknown parameters for constructing local volatility surface with $M_s = 10$ and (b) the local volatility surface constructed by interpolation with $\{\sigma_1^*, \ldots, \sigma_{M_s}^*\} = \{0.20,\ 0.12,\ 0.09,\ 0.15,\ 0.08,\ 0.07,\ 0.11,\ 0.05,\ 0.05,\ 0.07\}$.

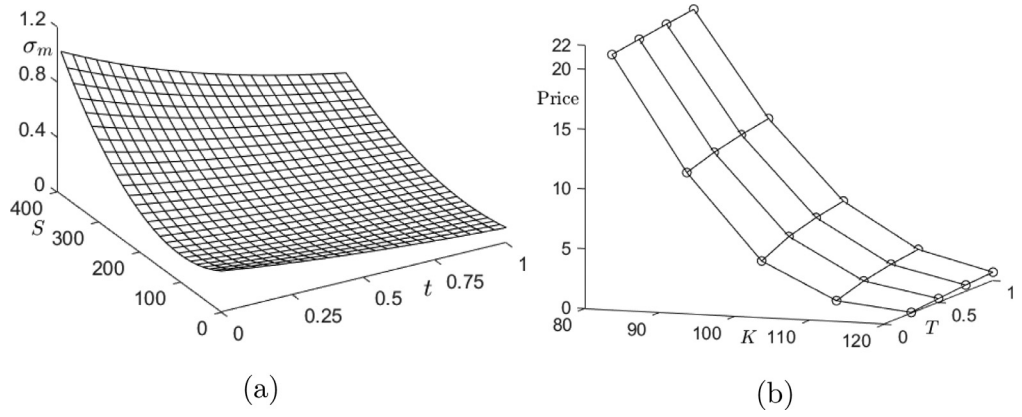

Fig. 5. (a) Given LV surface $\sigma_m(S,t)$, Eq. (9) and (b) European call option prices V_α^β with the given LV surface.

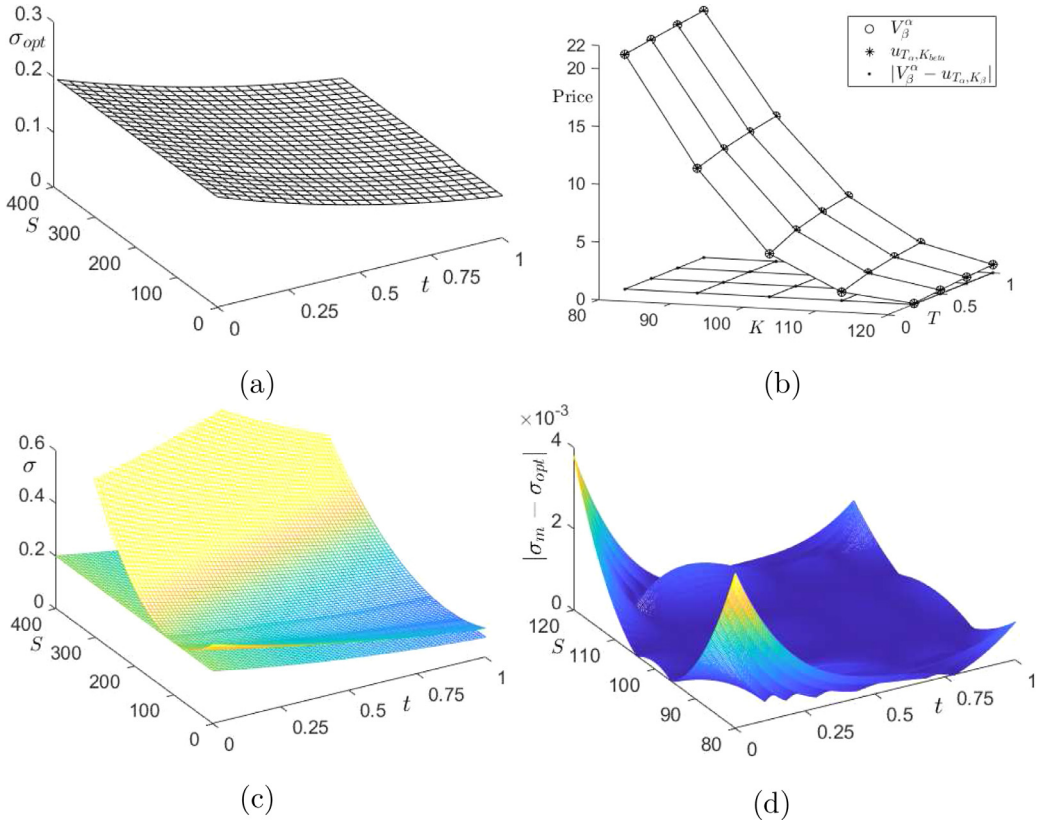

Fig. 6. (a) Optimal LV surface. (b) Plots of V_β^α, u_{T_α,K_β}, and $|V_\beta^\alpha - u_{T_\alpha,K_\beta}|$. (c) Mesh plots of $\sigma_m(S,t)$ and $\sigma_{opt}(S,t)$. (d) Mesh plot of $|\sigma_m(S,t) - \sigma_{opt}(S,t)|$.

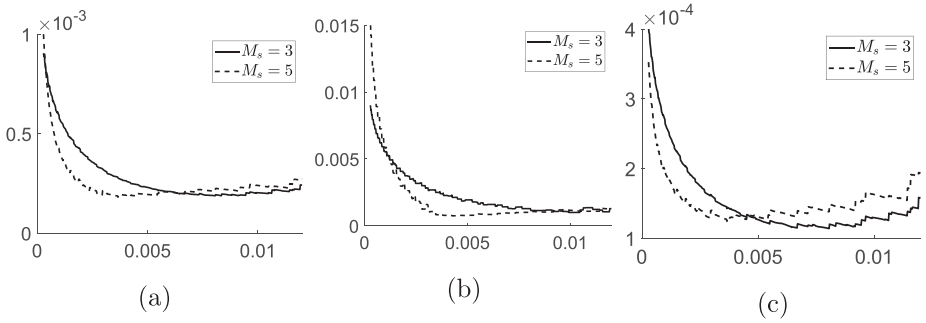

Fig. 7. Plot of the accuracy of the proposed method for size of influential region and the number of the unknown value. (a) RMSE, (b) MAE, and (c) AME.

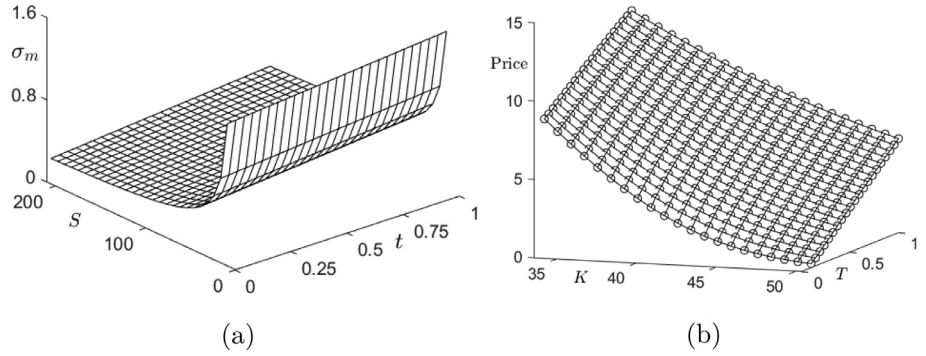

Fig. 8. (a) Given LV surface $\sigma_m(S,t)$ and (b) European call option prices V_α^β with the given volatility function (10).

curve-fitting solver in the least-squares sense:

$$\sigma_{im} = \text{lsqcurvefit}('\text{BSequation}', \sigma_{im}{}^0, (1,\ldots,M_k \times M_t), V, lb) \quad (7)$$

where σ_{im} and σ_{im}^0 are the optimal and initial constant implied volatility, respectively, *'BSequation'* returns the exact or numerical solution of Eq. (3) at (T_α, K_β) for $\alpha = 1,\ldots,M_t,\ \beta = 1,\ldots,M_k$, $V = [V_1^1\ V_1^2\ \ldots\ V_{M_t}^{M_k}]$ is the vector with the market prices, and lb is a lower bound constraint. The volatility is nonnegative; therefore, we set $lb = 0$.

Step 2: We determine the influential region for the computational domain. Kim et al. [23] investigated the domain of influence of the LV function using a Monte Carlo simulation (MCS). However, the MCS method has a problem with high computational cost, therefore, we use the probability density function (PDF) of a log-normal distribution to find the influential region with the constant implied volatility σ_{im}. Fig. 3 shows the PDF of the log-normal distribution with $r = 0.0066$, $T = 1$, $\sigma_{im} = 0.1888$, and $S_0 = 389.29$.

$$f(S,t) = \frac{1}{\sigma_{im} S\sqrt{2\pi t}} \exp\left(-\frac{[\ln(S/S_0) - (r - \sigma_{im}^2/2)t]^2}{2\sigma_{im}^2 t}\right). \quad (8)$$

Step 3: We estimate a time-dependent volatility (TDV) function $\sigma_{TDV}(t)$ using the algorithm proposed in Jin et al. [5]. Refer to Jin et al. [5] for details of the algorithm.

Step 4: To find the optimal LV surface, we use Eq. (6). The LV surface is constructed by cubic spline interpolation with constant volatilities $\sigma_1^*,\ldots,\sigma_{M_s}^*$ in the area of influence, maturity T_α, and present value S_0, where the number of unknown values is $M_s = n_s(M_t - 1) + 1$. Here, n_s is an odd number. Fig. 4(a) illustrates the position of unknown volatilities for constructing the LV surface with $M_s = 10$. Fig. 4(b) shows the LV surface constructed by interpolation with $\{\sigma_1^*,\ldots,\sigma_{M_s}^*\} = \{0.20, 0.12, 0.09, 0.15, 0.08, 0.07, 0.11, 0.05, 0.05, 0.07\}$.

To find $\sigma(S,t)$, we use *lsqcurvefit* to minimize Eq. (6). To avoid having a negative value when we use *lsqcurvefit* to find the optimal constant volatilities $\sigma_1^*,\ldots,\sigma_{M_s}^*$, we use the lower bound constraint $lb = 0$. Here, the time-dependent volatility function $\sigma_{TDV}(t)$ is used as the initial guess value.

The pseudocode in Algorithm 1 describes the proposed reconstruction algorithm for the LV function.

Table 1
European call option prices generated by the given LV surface (9).

K_β	80	90	100	110	120
$T_1 = 90/360$	20.3149	10.7845	3.7181	0.7342	0.0867
$T_2 = 180/360$	20.6774	11.5584	4.8532	1.4707	0.3319
$T_3 = 270/360$	21.0317	12.1216	5.5277	1.9526	0.5491
$T_4 = 360/360$	21.3623	12.5590	5.9901	2.2839	0.7138

3. Numerical experiments

We demonstrate the performance of the proposed algorithm for constructing LV surface by several numerical experiments.

3.1. Test problem 1

We consider the following nonlinear LV surface [25]:

$$\sigma_m(S,t) = [0.2 + 10^{-5}(S - 100)^2]e^{-t} \quad (9)$$

for $(S,t) \in [0, 400] \times (0, 1]$. First, we obtain the market price V_β^α of the European call option using the given LV surface (9) by solving (4) with the maturity time $T_\alpha = 90\alpha/360$ for $\alpha = 1, 2, 3, 4$ and strike prices $K_\beta = 70 + 10\beta$ for $\beta = 1, 2, \ldots, 5$. The parameters are set as follows: the risk-free rate $r = 0.03$, the spot price $S_0 = 100$, $N_s = 401$, and $N_\tau = 401$. The European option prices generated in Eq. (9) are represented in Table 1. Fig. 5 shows the given LV surface and option prices.

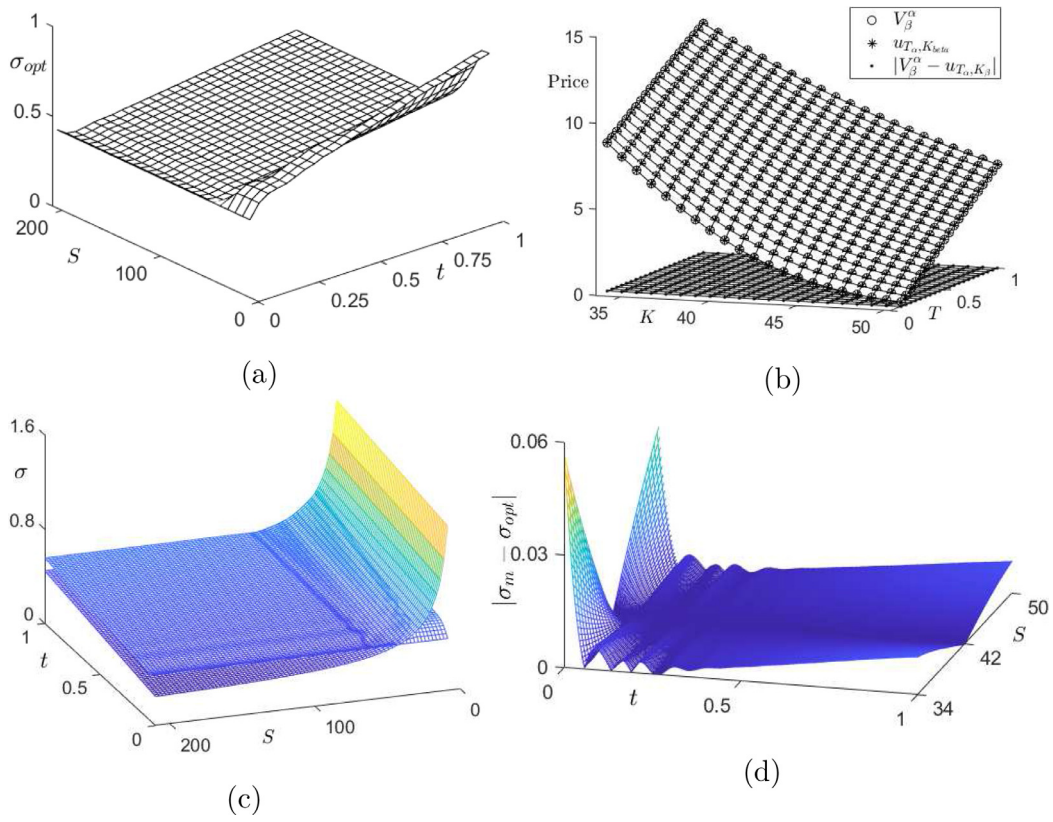

Fig. 9. (a) Optimal LV surface. (b) Plots of V_β^α, u_{T_α,K_β}, and $|V_\beta^\alpha - u_{T_\alpha,K_\beta}|$. (c) Mesh plots of $\sigma_m(S,t)$ and $\sigma_{opt}(S,t)$. (d) Mesh plot of $|\sigma_m(S,t) - \sigma_{opt}(S,t)|$ in the strike region.

Table 2
RMSE, MAE, and AME for different levels and the number of unknown value M_s.

Level		0.006	0.007	0.008	0.009	0.010
$M_s = 3$	RMSE	2.0925E−4	1.9508E−4	1.8837E−4	1.9082E−4	2.0256E−4
	MAE	1.5928E−3	1.2916E−3	1.2790E−3	1.1764E−3	0.9934E−3
	AME	1.2137E−4	1.1775E−4	1.1428E−4	1.1765E−4	1.2938E−4
Level		0.0062	0.0064	0.0066	0.0068	0.0070
$M_s = 5$	RMSE	2.0528E−4	1.9944E−4	1.9832E−4	1.9921E−4	1.9508E−4
	MAE	1.5928E−3	1.4585E−3	1.5448E−3	1.4134E−3	1.2916E−3
	AME	1.1919E−4	1.1675E−4	1.1537E−4	1.1969E−4	1.1775E−4

Next, using the proposed algorithm, we find the optimal LV surface $\sigma_{opt}(S,t)$ that minimizes Eq. (6). We use $M_s = 10$ and level 0.008 of the PDF for the influential region.

Fig. 6 represents (a) optimal LV surface and (b) plots of V_β^α, u_{T_α,K_β}, and $|V_\beta^\alpha - u_{T_\alpha,K_\beta}|$. Fig. 6(c) and (d) compare the optimal LV surface $\sigma_{opt}(S,t)$ with the given LV function $\sigma_m(S,t)$. The root mean square error (RMSE), mean absolute error (MAE), and absolutely maximum error (AME) in the influential region between $\sigma_{opt}(S,t)$ and $\sigma_m(S,t)$ are approximately 0.0002, 0.0013, and 0.0001, respectively. The proposed algorithm is sufficiently accurate for recovering the exact volatility function.

3.2. Parameter effect

In this section, we consider the effect of the size of the influential domain and the number of unknown values on the accuracy of the proposed method. We set the same conditions as those in Section 3.1. When $M_s = 3$ and $M_s = 5$, Fig. 7(a)–(c) show RMSE, MAE, and AME for each level of the PDF of the influential region, respectively.

Table 2 lists the RMSE, MAE, and AME for the level $\{0.006, 0.007, 0.008, 0.009, 0.010\}$ of the PDF for the influential region with $M_s = 3$ and the level $\{0.0032, 0.0034, 0.0036, 0.0038, 0.0040\}$ with $M_s = 5$. The level 0.008 with $M_s = 3$ and level 0.0066 with $M_s = 5$ are sufficiently accurate.

3.3. Test problem 2

For the second LV surface, we compare the performance with another algorithm [24,25] to construct the LV for the underlying asset and time. In [24], the authors used the following LV surface to verify the performance of their algorithm:

$$\sigma_m(S,t) = \sigma_A + \frac{A}{S} + Bt, \quad (0.2S_0 \le S \le 5S_0,\ 0 \le t \le 1), \tag{10}$$

where $A = 10$, $B = 0.2$, and $\sigma_A = 0.2$. The parameters are set as: the maturity time $T_\alpha = 0.1 + 0.045\alpha$ for $\alpha = 0, 1, \ldots, 20$ and the strike prices $K_\beta = 33.6 + 0.84\beta$ for $\beta = 0, 1, \ldots, 20$, $r = 0.05$, $q = 0.03$, $S_0 = 42$, $N_s = 401$, and $N_\tau = 401$. Fig. 8(a) and (b) show the

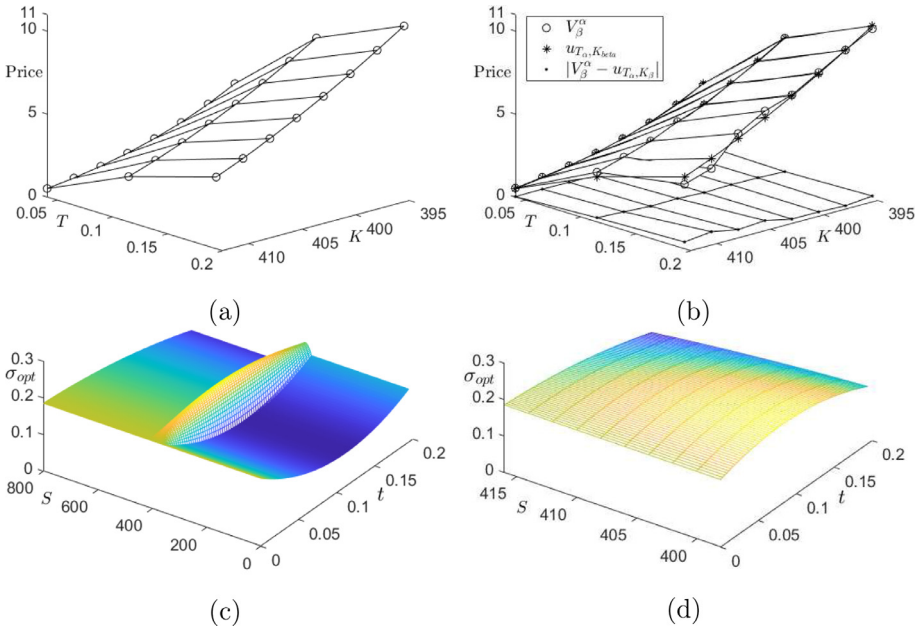

Fig. 10. (a) KOSPI 200 call option prices. (b) Plots of V_β^α, u_{T_α,K_β}, and $|V_\beta^\alpha - u_{T_\alpha,K_\beta}|$. (c) Optimal LV surface. (d) Mesh plots of $\sigma_{opt}(S,t)$ in the strike region.

Table 3
European call option prices of KOSPI 200 index on from January 2021 to March 2021 on 30 December 2020 with respect to the strike and maturity.

K_β	395	397.5	400.0	402.5	405.0	407.5.0	410.0	412.5
$T_1 = 15\Delta\tau$	3.70	2.95	2.31	1.79	1.35	1.02	0.76	0.54
$T_2 = 42\Delta\tau$	8.06	7.03	6.11	5.33	4.75	4.02	3.49	3.01
$T_3 = 71\Delta\tau$	10.25	9.4	8.48	7.56	7.03	6.1	4.42	3.91

Table 4
Numerical solution at the spot price S_0 and absolute errors between the numerical values and the KOSPI 200 index European call option prices on from January 2021 to March 2021 on 30 December 2020.

K_β	395	397.5	400.0	402.5	405.0	407.5.0	410.0	412.5
$T_1 = 15\Delta\tau$	3.8046	3.0038	2.3299	1.7891	1.3483	0.9951	0.7175	0.5127
	(0.1046)	(0.0538)	(0.0199)	(0.0009)	(0.0017)	(0.0249)	(0.0425)	(0.0273)
$T_2 = 42\Delta\tau$	8.0740	7.1065	6.2059	5.3820	4.6232	3.9290	3.2995	2.7462
	(0.0140)	(0.0765)	(0.0959)	(0.0520)	(0.1268)	(0.0910)	(0.1905)	(0.2638)
$T_3 = 71\Delta\tau$	10.4195	9.3849	8.4019	7.4793	6.6095	5.7936	5.0336	4.3427
	(0.1695)	(0.0151)	(0.0781)	(0.0807)	(0.4205)	(0.3064)	(0.6136)	(0.4327)

given LV surface $\sigma_m(S,t)$ and the European option prices V_β^α, respectively.

To find the optimal LV surface $\sigma_{opt}(S,t)$, we use $M_s = 10$ and the level 0.007 of the PDF for the influential region.

Fig. 9 represents (a) optimal LV surface and (b) plots of V_β^α, u_{T_α,K_β}, and $|V_\beta^\alpha - u_{T_\alpha,K_\beta}|$. Fig. 9(c) and (d) compare the optimal LV surface $\sigma_{opt}(S,t)$ with the given LV function $\sigma_m(S,t)$. The AME of the LV in the previous study was 0.02 [24] and 0.08 [25]. However, the AME in the influential region from the proposed algorithm is 0.0189, which points out the superior performance of the proposed method.

3.4. KOSPI 200 index call option

For real-market applications, we construct the LV surface using the proposed method with the European call option prices of the KOSPI 200 index from January 2021 to March 2021 on 30 December 2020. Table 3 lists the European call option prices for the strike $K_\beta = 395 + 2.5(\beta - 1)$ for $\beta = 1, 2, \ldots, 8$ and maturity $T_1 = 15\Delta\tau$, $T_2 = 42\Delta\tau$, and $T_3 = 71\Delta\tau$ with $\Delta\tau = 1/365$, see Fig. 10(a). At this time, the spot value and the risk-free rate are $S_0 = 389.29$ and $r = 0.0066$, respectively.

We use $M_s = 10$ and level 0.008 of the PDF for the influential region. We construct the optimal LV surface $\sigma(S,t)$ by applying the proposed method using real market option data, as shown in Fig. 10. Table 4 represents the numerical option prices by the constructed optimal LV surface and the European call option prices at $t = T_1$, T_2, and T_3.

Fig. 10 (b) represents the comparison between real market prices V_β^α and the computed prices u_{T_α,K_β}, which are calculated by the optimal LV; (c) shows the mesh plot of $\sigma_{opt}(S,t)$; and (d) shows the optimal LV $\sigma_{opt}(S,t)$ in the strike region. Table 4 presents the numerical results; and the absolute errors between the numerical values and the European call option prices of KOSPI 200 index in parentheses.

Algorithm 1 Reconstructing the LV surface using the *lsqcurvefit*.

S_0: Present value of underlying asset, M_s: The number of unknown parameters
$T_1 < \ldots < T_\alpha < \ldots < T_{M_t}$: Maturity time
$K_1 < \ldots < K_\beta < \ldots < K_{M_k}$: Strike price
$V = [V_1^1, \ldots, V_\beta^\alpha, \ldots, V_{M_k}^{M_t}]$: Market price
▷ Find the optimal constant implied volatility σ_{im}
$\sigma_{im} = lsqcurvefit('BSequation', \sigma_{im}^0, (1, \ldots, M_k \times M_t), V, lb)$, where $'BSequation'$ returns the exact solution of Eq. (3) for European call option
▷ Find the influential region using Eq. (8)
for $i = 1$ to $M_t - 1$ **do**
$(L_i, R_i) = \underset{S}{\operatorname{argmin}} |(f(S, (T_i + Ti + 1)/2) - Lv|$, Lv: level of PDF
end for
▷ Positioning of unknown parameters σ_i for $i = 1, \ldots, M_s$, $M_s = n_s(M_t - 1) + 1$.
for $i = 1$ to $M_t - 1$ **do**
$t = (T_i + T_{i+1})/2$, $\sigma(0, t) = \sigma_{(i-1)n_s+2}$, $\sigma(S_0, t) = \sigma_{in_s}$, $\sigma(S_{max}, t) = \sigma_{in_s+1}$
for $j = 1$ to $(n_s - 1)/2$ **do**
$dL = (S_0 - L_i)/(n_s - 1)$, $dR = (R_i - S_0)/(n_s - 1)$
$\sigma(L_i + dL(j-1), t) = \sigma_{(i-1)n_s+j+1}$, $\sigma(R_i - dR(j-1), t) = \sigma_{in_s-j+2}$
end for
end for
▷ Find the TDV function $\sigma_{TDV}(t)$
$\sigma_{TDV} = lsqcurvefit('BSequation', \sigma_{TDV}^0, (1, \ldots, M_k \times M_t), V, lb)$.
▷ Find optimal value of unknown parameters σ^*
$\sigma^* = lsqcurvefit('BSequation', \sigma_{TDV}, (1, \ldots, M_k \times M_t), V, lb)$.
▷ Reconstruct the LV surface by cubic spline interpolation over time and space: $\sigma_{loc}(S, t) = interp2(X_{\sigma^*}, Y_{\sigma^*}, \sigma^*, \hat{S}, \hat{t}, 'spline')$,
where X_{σ^*} and Y_{σ^*} are 2D grid coordinates based on the coordinates of σ^*. In addition, $\hat{S}$ and $\hat{t}$ are 2D grid coordinates based on S and t, respectively.

4. Conclusions

We developed a numerical method for the robust and accurate construction of the LV surface for European options in an unknown parametric approach by using the BS equation. The LV function is one of the most important functions of pricing options in financial markets. The finding of the LV function is an ill-posed inverse problem. To overcome this difficulty, the first step in the proposed numerical algorithm is to estimate the constant implied volatility using the exact formula of the European call option and the nonlinear curve-fitting solver, and then we use the PDF of the log-normal distribution to find the influential region with constant implied volatility. Next, we compute the TDV function, which is used as an initial value for the fast estimation of unknown variability that constructs the LV surface. Finally, we use an implicit Euler scheme to numerically solve the BS equation and a nonlinear fitting function to compute the LV surface. We performed computational experiments using synthetic and real market data. The numerical results demonstrate the robust and accurate construction of the LV surface using the proposed method.

Declaration of Competing Interest

The authors declare that they have no known competing financial interests or personal relationships that could have appeared to influence the work reported in this paper.

CRediT authorship contribution statement

Sangkwon Kim: Conceptualization, Writing - original draft, Investigation, Methodology, Software, Writing - review & editing. **Junseok Kim:** Conceptualization, Investigation, Methodology, Validation, Project administration, Funding acquisition, Writing - review & editing.

Acknowledgment

The corresponding author (J.S. Kim) was supported by the Brain Korea 21 FOUR from the Ministry of Education of Korea. The authors are grateful to the reviewers for their contributions to improve this paper.

References

[1] Bustamante M, Contreras M. Multi-asset Black–Scholes model as a variable second class constrained dynamical system. Phys A 2016;457:540–72.
[2] Khodayari L, Ranjbar M. A computationally efficient numerical approach for multi-asset option pricing. Int J Comput Math 2019;96:1158–68.
[3] Black F, Scholes M. The pricing of options and corporate liabilities. J Polit Econ 1973;81:637–54.
[4] Bianchi ML, Rachev ST, Fabozzi FJ. Calibrating the italian smile with time-varying volatility and heavy-tailed models. Comput Econ 2018;3(51):339–78.
[5] Jin Y, Wang J, Kim S, Heo Y, Yoo C, Kim Y, et al. Reconstruction of the time-dependent volatility function using the Black–Scholes model. Discrete Dyn Nat Soc 2018;2018:1–9 3093708. doi: 10.1155/2018/3093708.
[6] Dupire B. Pricing with a smile. Risk 1994;1(7):18–20.
[7] Derman E, Kani I. Stochastic implied trees: Arbitrage pricing with stochastic term and strike structure of volatility. Int J Theor Appl Finance 1998;01(1):61–110.
[8] Dumas B, Luciano E. From volatility smiles to the volatility of volatility. Decis Econ Finance 2019;2(42):387–406.
[9] Achdou Y. An inverse problem for a parabolic variational inequality arising in volatility calibration with american options. SIAM J Control Optim 2005;5(43):1583–615.
[10] Zeng YH, Wang SL, Yang YF. Calibration of the volatility in option pricing using the total variation regularization. J Appl Math 2014;2014:1–9 510819. doi: 10.1155/2014/510819.
[11] Deng G. Pricing perpetual american floating strike lookback option under multiscale stochastic volatility model. Chaos Solitons Fractals 2020;141:110411.
[12] Lin S, He XJ. A closed-form pricing formula for forward start options under a regime-switching stochastic volatility model. Chaos Solitons Fractals 2021;144:110644.
[13] A. Itkin. Fitting Local Volatility: Analytic and Numerical Approaches in Black-Scholes and Local Variance Gamma Models. Number 11623. World Scientific Publishing Co. Pte. Ltd., 2020.
[14] Guo I, Loeper G, Wang S. Local volatility calibration by optimal transport. In: In 2017 MATRIX annals. Cham: Springer; 2019. p. 51–64.
[15] Lim H.. Improved methods for implied volatility surface and implied distributions. 2020. Available at SSRN. 3561100
[16] Xu Z, Jia X. The calibration of volatility for option pricing models with jump diffusion processes. Appl Anal 2019;4(98):810–27.
[17] Ogetbil O., Ganesan N., Hientzsch B.. Calibrating local volatility models with stochastic drift and diffusion. 2020. Available at SSRN. 3702442
[18] Santos AA. Bayesian estimation for high-frequency volatility models in a time deformed framework. Comput Econ 2021;57:455–79.
[19] Tavella D, Randall C. Pricing financial instruments: the finite difference method. New York: Jone Wiely and Sons; 2000.
[20] Windfcliff H, Forsuth PA, Vetzal KR. Analysis of the stability of the linear boundary condition for the Black–Scholes equation. J Comput Finance 2004;8:65–92.
[21] Thomas L. Elliptic problems in linear differential equations over a network: Watson scientific computing laboratory. New York: Columbia Univesity; 1949.
[22] Nabi KN, Kumar P, Erturk VS. Projections and fractional dynamics of COVID-19 with optimal control strategies. Chaos Solitons Fractals 2021;145:110689.
[23] Kim H, Kim S, Han H, Jang H, Lee C, Kim J. Domain of influence of local volatility function on the solutions of the general Black–Scholes equation. Pure Appl Math 2020;1(27):43–50.
[24] Boyle S, Thangaraj PP. Volatility estimation from observed option prices. Decis Econ Finance 2000;1(23):31–52.
[25] Kim S, Han H, Jang H, Jeong D, Lee C, Lee W, et al. Reconstruction of the local volatility function using the Black–Scholes model. J Comput Sci 2021:101341.